Fusion of Multiresolution Seismic Tomography Maps Using Physics-informed Probability Graphical Models

Zheng Zhou[1]; Peter Gerstoft[1]; Kim Olsen[2]

[1]University of California, San Diego; [2]San Diego State University

Abstract

Fusing tomography models with different resolutions is desired when updating community models, to enable more accurate ground motion simulations. Toward this goal, we introduce a novel approach called the Physics-Informed Probability Graphical Model (PIPGM) designed to integrate seismic models with varying resolutions and uneven data point distributions. The PIPGM is able to capture relationships between subdomains of multiple resolutions, such as well-defined high-resolution (HR) embedded into low-resolution (LR) regions. We assess the efficacy of the proposed methodology using both 2D and 3D velocity models, including synthetic checkerboard models as well as a fault zone model derived from the 2019 Ridgecrest, CA, earthquake sequence. Our findings demonstrate a ~38% reduction in travel time residuals compared to conventional Gaussian kernel smoothing in the 2D experiments, with similar reductions expected in 3D. Our proposed PIPGM holds significant potential for enhancing our understanding of Earth's structure and offers promising advancements in other seismic research applications, such as earthquake ground motion prediction.

Motivation and Objective

- Combining models with different resolutions is an essential step for updating community models.
- A direct merging will preserve the sharp changes on boundary areas (a2), while a strong smoothing will lose the detailed information from HR models (a3).
- We propose a probability graphical model to adaptively balance the trade-off between smoothness and sharp details.

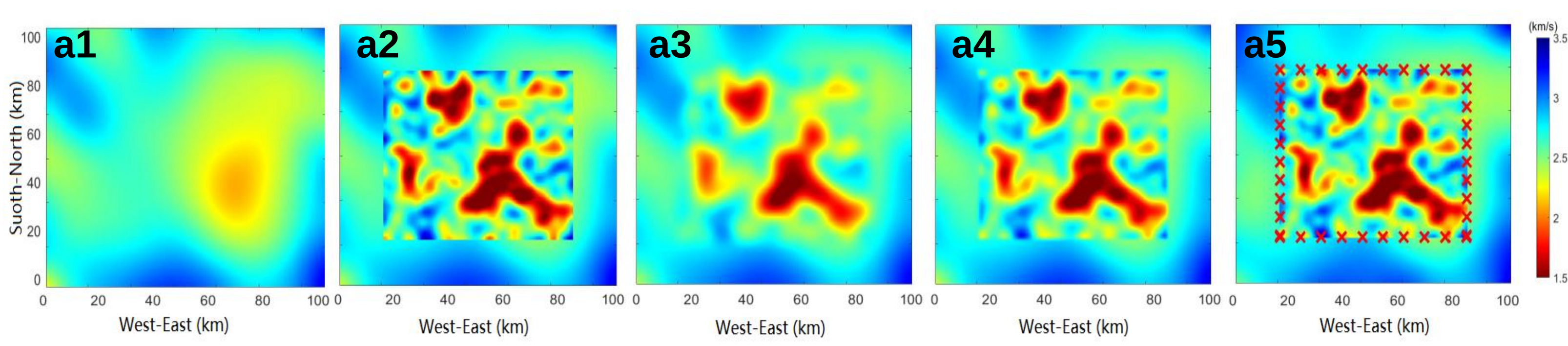

Figure (a1) The LR SCEC CVM-S4.26 [4] around the Ridgecrest area. **(a2)** Directly superimposing the velocity models from HR 1 Hz Rayleigh wave tomography (top 1 km depth, converted to S-wave velocity) and the LR CVM model. **(a3)** Smoothed by 7x7 Gaussian kernel filter. **(a4)** Fused by our PIPGM method. **(a5)** Synthetic sensors ('X') are placed in the boundary areas to calculate travel time residuals. We use travel time Root-Mean-Squared-Error (RMSE, which measures how much information is lost after model fusion [3]) to evaluate our tomography model fusion results.

Markov Random Field

A Markov random field can consider the geometric property and balance between smoothness and sharpness (detailed information) in images [2].

Let $A_{i,j}$ be the observed velocity value (continuous), and $X_{i,j}$ be the hidden label (discrete). We assume $A_{i,j}$ follows the distribution approximated by a weighted-Gaussian distribution, so that we iteratively solve the following problems with Expectation–maximization (EM) and Markov chain Monte Carlo (MCMC) algorithm:

$$X^*_{i,j} = \arg\max_{X_{i,j}} p(X_{i,j} \mid A_{i,j}) = \arg\min_{X_{i,j}} \omega_{i,j}\underbrace{\boxed{\theta_0(X_{i,j}, A_{i,j})}}_{\text{Data Cost}} + \sum_{(i',j')\in\mathcal{N}_{i,j}} \omega_{i',j'}\underbrace{\boxed{\theta_1(X_{i,j}, X_{i',j'})}}_{\text{Smoothness Cost}} + C.$$

$$A_{i,j} \sim \sum_{n=1}^{6} P(X_{i,j}=n)N(\mu_n, \sigma_n^2)$$

$\omega_{i,j}$ is a weight term related to physical information (ray-path density and gradients), μ_n and σ_n^2 are the mean and variance of all the pixels with hidden label n. C is a bias constant which only depends on the model setting. Index (i', j') represents the neighboring pixels of pixel (i, j).

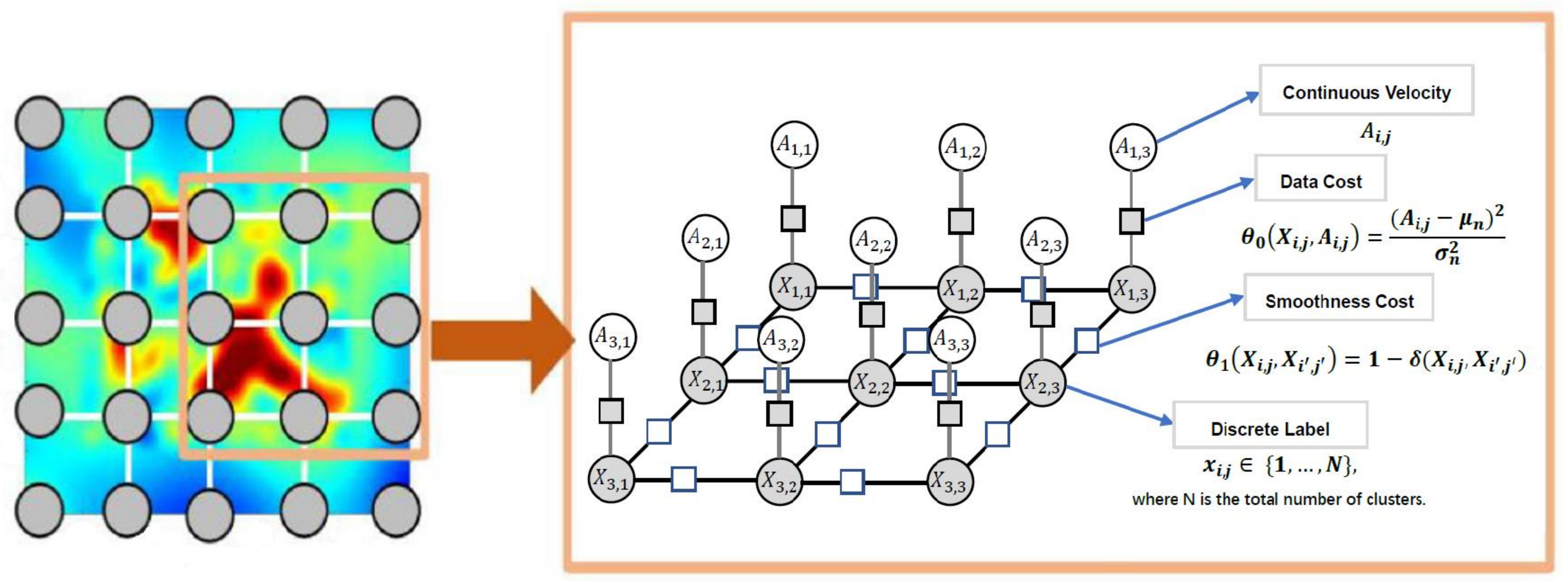

Figure (b) Each pixel has a continuous velocity value $A_{i,j}$ and a discrete label $X_{i,j}$. The objective function designed for model fusion has two parts: (1) the data cost θ_0 that forces the pixels with the same label to follow the same Gaussian distribution, and (2) the smoothness cost θ_1 that promotes the smoothness among neighboring pixels.

Results

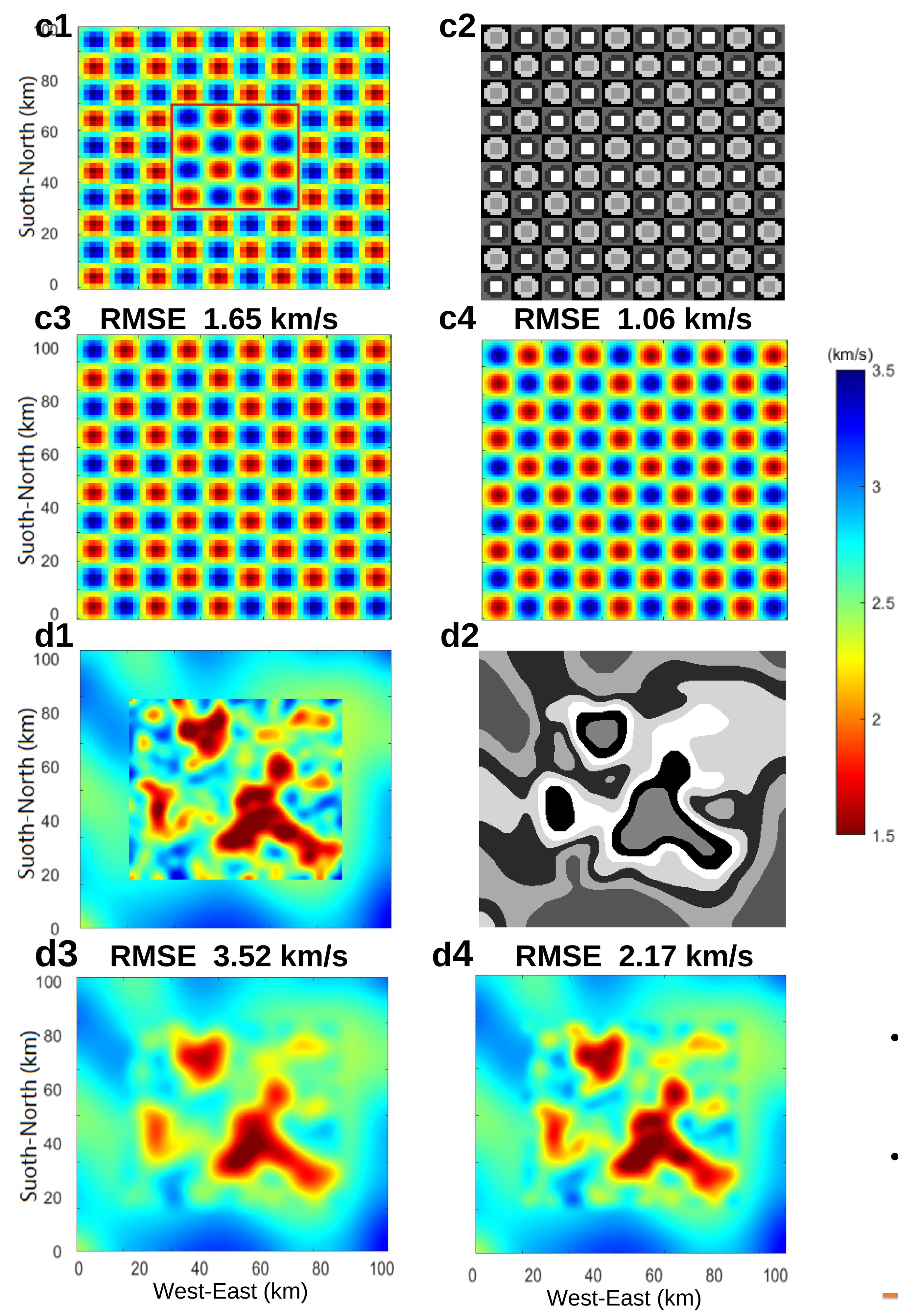

Figure (c1-c4) Checkerboard and **(d1-d4)** Ridgecrest 2D models. **(c1, d1)** Superimposed HR and LR models. **(c2, d2)** 6-class label mask maps for HR models (pixels with the same label are learned together). **(c3, d3)** Smoothing results with a 7×7 Gaussian kernel filter. **(c4, d4)** Fusion results with our PIPGM method. The emulation results show that our PIPGM achieves smaller RMSE results, indicating smaller information loss.

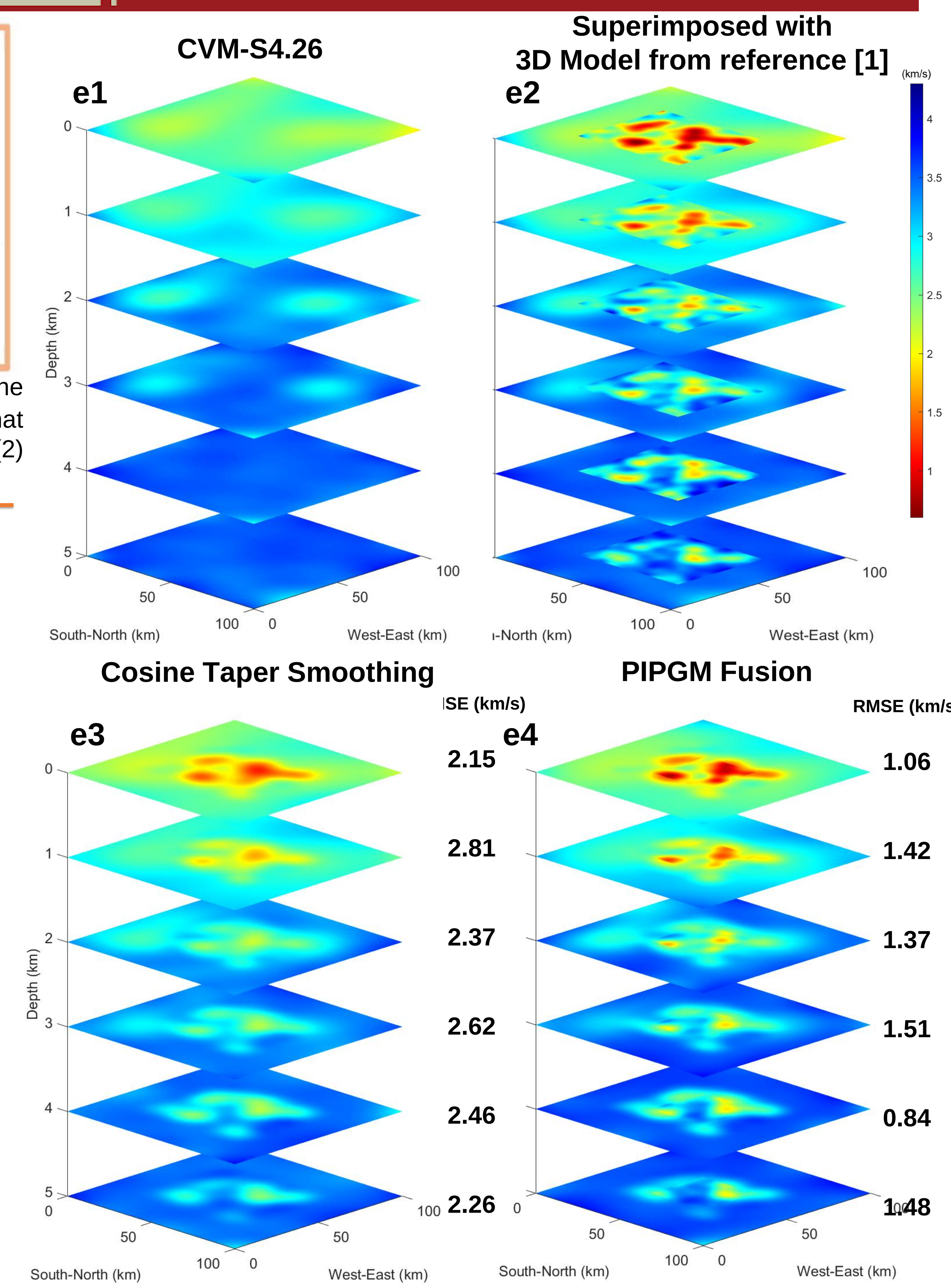

Figure (e1-e4) Ridgecrest 3D models. (**e1**) The LR 0-5 km depth S-wave velocity model from CVM-S4.26 around the Ridgecrest area. **(e2)** Direct superposition of the HR model from surface wave dispersion inversion [1] and the LR CVM-S4.26. **(e3)** Fusion results with cosine taper smoothing. **(e4)** Fusion results with our PIPGM method. Our PIPGM removes the discontinuous changes on boundary areas and adaptively preserves sharp patterns from HR models. This results in a significant reduction in RMSE errors.

Conclusion

- Our PIPGM-based tomography model fusion method achieves a balance between smoothing undesired sharp boundaries and preserving detailed information from HR models.
- Currently, our proposed model informs physical and seismological information (ray-path density and the gradient of tomography models) as prior knowledge for MRF weights. The physics-based constraints produce improved interpretation of the fusion results.

References

[1] Zhou, Z., Bianco, M., Gerstoft, P. and Olsen, K., 2022. High-Resolution Imaging of Complex Shallow Fault Zones Along the July 2019 Ridgecrest Ruptures. Geophysical Research Letters, 49(1).

[2]. Li, S.Z., 2009. Markov random field modeling in image analysis. Springer Science & Business Media.

[3]. Mackens S, Albers W, Fechner T, Tweeton D, Karl L. Interpretation of seismic tomography results using data quality and residual error maps. InSymposium on the Application of Geophysics to Engineering and Environmental Problems 2014 2014 Mar 20 (pp. 79-84).

[4]. Taborda, R., S. Azizzadeh-Roodpish, N. Khoshnevis, and K. Cheng (2016), Evaluation of the southern California seismic velocity models through simulation of recorded events, Geophys. J. Int., 205, 1342-1364, doi:10.1093/gji/ggw085.

Acknowledgements

The research is supported by SCEC awards 22053 and 21133.